Parkinsonism and Related Disorders 33 (2016) 58–64

Contents lists available at ScienceDirect

Parkinsonism and Related Disorders

journal homepage: www.elsevier.com/locate/parkreldis

Altered functional connectivity in the default mode network is associated with cognitive impairment and brain anatomical changes in Parkinson's disease

Olaia Lucas-Jiménez [a], Natalia Ojeda [a], Javier Peña [a], María Díez-Cirarda [a], Alberto Cabrera-Zubizarreta [b], Juan Carlos Gómez-Esteban [c], María Ángeles Gómez-Beldarrain [d], Naroa Ibarretxe-Bilbao [a, *]

[a] Department of Methods and Experimental Psychology, Faculty of Psychology and Education, University of Deusto, Bilbao, Spain
[b] OSATEK, MR Unit Hospital of Galdakao, Galdakao, Usansolo, Spain
[c] Neurodegenerative Diseases Group, Biocruces Health Research Institute, University of Basque Country, Barakaldo, Spain
[d] Department of Neurology, Hospital of Galdakao, Galdakao, Usansolo, Spain

ARTICLE INFO

Article history:
Received 27 April 2016
Received in revised form
2 September 2016
Accepted 9 September 2016

Keywords:
Parkinson's disease
Default mode network
Functional connectivity
Gray matter
Diffusion-weighted imaging
Cognitive impairment

ABSTRACT

Objective: To assess whether functional neural connectivity is disrupted between the regions of the default mode network (DMN) in Parkinson's disease (PD) and how this connectivity is related to cognition, brain gray matter structure and white matter integrity and diffusivity.
Methods: Thirty-seven PD patients and 16 healthy controls were evaluated, using resting-state functional magnetic resonance imaging (MRI), T1-weighted MRI, diffusion-weighted imaging and a battery of cognitive tests. Functional connectivity between the regions of the DMN, specifically in the precuneus, anterior and posterior cingulate, medial prefrontal and temporal and inferior parietal cortices was assessed with seed-to-voxel connectivity; gray matter volume and white matter values were determined using voxel-based morphometry and tract-based spatial statistics.
Results: Reduced functional connectivity was observed between the posterior cingulate and medial temporal lobe in PD. Lower cognitive performance, gray matter loss in posterior, medial temporal and parietal areas, and fractional anisotropy reduction in the white matter adjacent to DMN regions were also observed in PD patients compared with healthy controls. Lower DMN functional connectivity correlated with lower verbal and visual memory and visual abilities performance in PD. In addition, lower DMN functional connectivity correlated with lower gray matter volume in the posterior cingulate and precuneus, and with lower white matter fractional anisotropy of the inferior longitudinal and posterior cingulate fasciculi in PD.
Conclusions: By combining different neuroimaging techniques and cognitive data, results showed that functional connectivity alteration between the regions of the DMN is associated with lower cognitive performance and gray and white matter abnormalities in PD.

1. Introduction

Parkinson's disease (PD) is a neurodegenerative disorder characterized by the progressive development of motor symptoms and cognitive decline, with dementia often occurring in advanced stages of PD [1]. Previously, PD has been related to deficits in executive functions, attention and visuospatial abilities but recent studies also showed that memory is a relevant cognitive deficit in this disease [2]. Previous studies have demonstrated brain anatomical changes [3], cognition task-related functional magnetic resonance imaging (fMRI) changes [4,5] and cognitive impairment in PD [6]. Recently, there has been growing interest in resting-state fMRI studies, as this approach allows the study of the brain's functional networks without requiring participants to perform any task. Moreover, high reproducibility of the findings supports the validity of resting-state fMRI outcome measures as biomarkers [7].

* Corresponding author. Faculty of Psychology and Education, University of Deusto, Avda Universidades 24, 48007, Bilbao, Spain.
E-mail address: naroa.ibarretxe@deusto.es (N. Ibarretxe-Bilbao).

http://dx.doi.org/10.1016/j.parkreldis.2016.09.012

The default mode network (DMN) is the most studied network in the resting-state and is derived from observations that specific brain regions are more active when the brain is in a wakeful resting-state than during the performance of external tasks. The areas that have been identified as part of the DMN are the medial prefrontal cortex (MPFC), anterior cingulate cortex (ACC), posterior cingulate cortex (PCC), precuneus, medial temporal lobe (MTL) and inferior parietal cortex (IPC) [8]. The relevance of the DMN has been emphasized in several neuropsychiatric diseases [8], but only a few studies have investigated the DMN in the context of PD [9–14]. FMRI studies have confirmed the crucial role played by the DMN in cognitive processing both in normal aging and neurodegenerative disorders [15,16]. In fact, the impairment of PCC and precuneus could be an important marker to distinguish amnestic mild cognitive impairment from healthy aging in the resting-state [17]. However, most neuroimaging studies assessing the DMN only had one single imaging modality making it difficult to investigate structural and functional changes in PD patients. Moreover, studies only assess global cognitive measure instead of extensive cognitive battery. To our knowledge, this is the first study assessing DMN disturbances and its cognitive and brain gray matter (GM) volume and white matter (WM) indexes correlates. Therefore, the first objective of this study was to investigate the resting-state functional connectivity (FC) between the regions of the DMN in PD patients, compared with healthy controls (HC). At the same time, we investigated cognitive differences, and GM volume and WM tracts differences in the DMN areas. The second objective was to explore the cognitive, GM volume and WM correlates of the DMN disturbances in PD. For the first objective, we hypothesized that PD patients would have lower FC, cognitive performance, GM volume and WM. For the second objective, we hypothesized that decreased FC in the DMN would be related to GM atrophy, lower WM, and diminished cognitive performance in PD.

2. Methods

2.1. Participants

The study included 37 PD patients recruited from the Department of Neurology at the Galdakao Hospital and from the PD Biscay Association (ASPARBI). We also included 16 HC who were acquaintances of the patients, matched with the patients by age, gender and years of education. PD patients were enrolled in the study if they fulfilled the UK PD Society Brain Bank diagnostic criteria, as assessed by a neurologist specialized in movement disorders. Other inclusion criteria were as follows: (i) age between 45 and 75 years; (ii) Hoehn and Yahr disease stage ≤ 3; and (iii) Unified PD Rating Scale (UPDRS) evaluated by the neurologist. The exclusion criteria were as follows: (i) the presence of dementia, as defined by the DSM-IV-R and the Movement Disorders Society clinical criteria for PD dementia; (ii) scores of <24 on the Mini Mental State Examination; (iii) the presence of other neurological illness or injury or atypical parkinsonism; (iv) unstable psychiatric disorders; (v) PD patients with visual hallucinations, as assessed by the Neuropsychiatric Inventory Questionnaire; and (vi) diagnosis of depression or a depression score of >5, as evaluated with the Geriatric Depression Scale. WM hyperintensity ratings were calculated twice by the same neuroradiologist using the Fazekas Scale based on T1-weighted images. One patient was taking no medication, and 36 were on anti-Parkinsonian treatment as follows: Levodopa (L-dopa) monotherapy (n = 4); combination of L-dopa and a dopamine agonist (n = 5); monoamine oxidase type B (MAO-B) inhibitors monotherapy (n = 1); combination of L-dopa and MAO-B (n = 5); combination of L-dopa, a dopamine agonist and MAO-B (n = 9); combination of dopamine agonist and MAO-B (n = 4); combination of a dopamine agonist and anticholinergics (n = 2); combination of glutamate agonists in combination with others (n = 4); and catechol-*O*-methyltransferase (COMT) inhibitors in combination with others (n = 2). Participants were symptomatically stable and evaluated during the "ON" period. Their Levodopa equivalent daily dose (LEDD) was registered. The clinical and sociodemographic characteristics of the study sample are shown in Table 1.

2.2. Ethics statement

The study protocol was approved by the Ethics Committee at the Health Department of the Basque Mental Health System in Spain. All subjects were volunteers and provided written informed consent prior to their participation in the study.

2.3. Cognitive evaluation

The cognitive battery included tests to evaluate processing speed, verbal fluency, verbal and visual learning and memory, visual abilities and executive functioning. All cognitive measures were converted into *z* scores, based on the pooled PD group, and all composite cognitive domains maintained satisfactory internal consistency. Processing speed (Cronbach $\alpha = 0.86$) was quantified, based on the Trail Making Test–A and Salthouse Letter Comparison Test. For verbal fluency ($\alpha = 0.89$), semantic and phonetic fluency tests were used. For verbal learning and memory ($\alpha = 0.92$), learning and long-term recall performance on the Hopkins Verbal Learning Test (version 2) was utilized. For visual learning and memory ($\alpha = 0.97$), learning and long-term recall performance on the Brief Visual Memory Test (version 1) was used. For visual abilities, the Drawing Test (order and copy) and Visual Objects and Space Perception Battery (incomplete letters and cubes) were used ($\alpha = 0.76$). Executive functioning ($\alpha = 0.73$) was determined, based on the WAIS-III Indirect digits and the Stroop test, using the word color and interference scores.

Table 1
Sociodemographic, clinical and neurological characteristics of the study sample.

	PD (n = 37)	HC (n = 16)	Statistics	*p*
Age (years)	67.97 (6.18)	65.13 (6.78)	$t = 1.45$	0.141
Gender (male)	22 (59.50%)	12 (75.00%)	$\chi^2 = 1.17$	0.279
Years of education	10.24 (4.81)	12.27 (4.30)	$t = -1.85$	0.069
Fazekas Scale	0.51 (0.69)	0.67 (0.90)	$\chi^2 = 2.89$	0.235
Fazekas 0	22 (59.46%)	10 (62.50%)		
Fazekas 1	11 (29.73%)	2 (12.50%)		
Fazekas 2	4 (10.81%)	4 (25.00%)		
UPDRS				
Mental State	1.86 (1.47)	–	–	–
Daily living activities	10.28 (6.27)	–	–	–
Motor exam	21.72 (10.29)	–	–	–
Treatment complications	2.75 (2.88)	–	–	–
Total score	36.61 (17.27)	–	–	–
LEDD	808.59 (536.81)	–	–	–
Years of disease evolution	6.96 (5.61)	–	–	–
Age of disease onset (years)	61.01 (8.44)	–	–	–
Hoehn and Yahr Scale	1.89 (.45)	–	–	–
Stage 1	5	–	–	–
Stage 1.5	3	–	–	–
Stage 2	26	–	–	–
Stage 2.5	1	–	–	–
Stage 3	2	–	–	–

Note: Values are expressed as the mean (Standard deviation), unless otherwise stated.
Abbreviations: PD = Parkinson's disease; HC = Healthy controls; UPDRS = Unified Parkinson Disease Rating Scale; LEDD = Levodopa Equivalent Daily Dose.

2.4. Image acquisition

Functional and structural imaging data were acquired on a 3-Tesla MRI machine (Philips-Achieva) at OSATEK, Hospital of Galdakao. All sequences were acquired during a single session. The resting-state fMRI was obtained in an axial orientation in an anterior-posterior phase direction, using a sequence sensitive to blood oxygen level-dependent (BOLD) contrast and a multislice gradient echo EPI sequence (TR = 2100 ms, TE = 16 ms, matrix size = 80 × 78 mm, flip angle = 80°, FOV = 240 × 240 × 130 mm, slice thickness = 3 mm, 214 slices, voxel size = 3.00 × 3.00 × 3.00 mm, acquisition time = 7 min 40 s). A T1-weighted images acquisition was obtained in a sagittal orientation (TR = 7.4 ms, TE = 3.4 ms, matrix size = 228 × 218 mm; flip angle = 9°, FOV = 250 × 250 × 180 mm, slice thickness = 1.1 mm, 300 slices, voxel size = 0.98 × 0.98 × 0.60 mm, acquisition time = 4 min 55 s). Diffusion-weighted images were obtained, in an axial orientation in an anterior–posterior phase direction, using a single-shot EPI sequence (TR = 7540 ms, TE = 76 ms, matrix size = 120 × 117 mm; flip angle = 90°, FOV = 240 × 240 × 132 mm, slice thickness = 2 mm, no gap, 66 slices, voxel size = 1.67 × 1.67 × 2.0 mm, acquisition time = 9 min 31 s) with two identical repetitions (32 uniformly distributed directions [b = 1000 s/mm2] and 1 b = 0 s/mm2).

2.5. Image pre-processing and analysis

2.5.1. Resting-state FC

Subjects were instructed not to engage in any particular cognitive or motor activity, to keep their eyes closed and not to fall asleep. Foam padding and earplugs were used to limit head movement and reduce scanner noise for the subjects. FC analysis were carried out using CONN Functional Connectivity Toolbox version 14.p [18]. First, functional images from each subject were realigned and unwarped, slice-timing corrected (interleaved bottom-up), coregistered with structural data, spatially normalized into the standard MNI space (Montreal Neurological Institute, Canada), outlier detected (ART-based scrubbing) and smoothed using a Gaussian kernel of 8 mm FWHM. All preprocessing steps were conducted using default preprocessing pipeline for volume-based analysis (to MNI-space). Structural data were segmented in GM, WM and cerebrospinal fluid (CSF), and normalized in the same default preprocessing pipeline. One major point is reducing the noise via the anatomical CompCor approach. This method extracts principal components (5 each) from WM and CSF time series. WM and CSF voxels are identified via a segmentation of the anatomical images. These components are added as confounds in the denoising step of the CONN toolbox [18]. The six head motion parameters derived from spatial motion correction were also added as confounds. As recommended band-pass filtering was performed with a frequency window of 0.008–0.09 Hz [19]. This preprocessing step was found to increase the retest reliability. Seed-to-voxel group comparisons were assessed using cluster-level inference at p(FWE) < 0.05 at a height threshold of p(uncorrected) < 0.001, as described in similar previous studies [13]. Seed-based analysis is the most commonly used approach in resting-state fMRI field when authors have a prior assumption. LEDD data was used as covariate in the analysis based on previous findings [13]. Seeds selected according to areas of the DMN [8] and based on Harvard-Oxford Structures Atlas (http://fsl.fmrib.ox.ac.uk/fsl/fslwiki/Atlases) were: (a) PCC, (b) ACC, (c) MPFC, (d) bilateral MTL, (e) bilateral IPC, and (f) precuneus. Post-hoc analyses were carried out to test whether FC differences and correlates were related to structural GM abnormalities. FC values of significant differences were obtained to perform statistical analyses in SPSS.

2.5.2. GM volume

Voxel-based morphometry (VBM) [20] analyses were carried out using the FMRIB Software Library (FSL) [21] tools (http://fsl.fmrib.ox.ac.uk/fsl/fslwiki/FSLVBM). First, a study-specific template was created, in order to register all images in the same stereotactic space (spatial normalization). To this aim, brain-extracted structural images were segmented into GM, WM and CSF. Then, GM images were affine registered to the GM ICBM-152 template and averaged to create an affine GM template. Next, GM images were re-registered to this affine GM template, using a non-linear registration, and averaged to create the study-specific nonlinear GM template in standard space. Second, individual GM images were registered nonlinearly to the study-specific template. After the normalization, the resulting GM images were modulated by multiplying with Jacobian determinants to correct for the volume change induced by the nonlinear spatial normalization. Finally, the images were smoothed with a sigma of 3.5 mm (8 mm FWHM). The DMN regions selected were described in resting-state FC section. Mean volume values of the regions of interest (ROI) were obtained to perform statistical analyses in SPSS.

2.5.3. WM indexes

Integrity and diffusivity data were preprocessed and analyzed using FSL [21]. First, images from each subject were concatenated and radiologically oriented. Then, the data were corrected for motion and eddy currents, the brain extraction tool (BET) was used and the diffusion gradients (bvecs) rotated to be corrected, thus providing a more accurate estimate of tensor orientations [22]. Then, all fractional anisotropy (FA) images were obtained by fitting a tensor model to the raw diffusion data, using FDT (DTIFIT). After, tract-based spatial statistics (TBSS) [23] was used for group comparisons. Using TBSS, the data were prepared to apply a nonlinear registration of all FA images into standard space. The mean FA image was created using a threshold of 0.2 and thinned to create a "mean FA skeleton" which represents the centres of all tracts common to the group. Axial diffusivity (AD) data were analyzed using "tbss non FA" script from TBSS, which applies the original non lineal registration to the AD data, merges all subjects warped AD data into a 4D file, then project this onto the original mean FA skeleton, and creates the 4D projected data. The same process was repeated for mean diffusivity (MD) and radial diffusivity (RD). Specific predefined WM ROIs associated with the DMN [24] were selected, based on the JHU White-Matter Tractography Atlas, as follows: (1) corpus callosum body, (2) anterior cingulate fasciculus, (3) posterior cingulate fasciculus, (4) inferior longitudinal fasciculus, and (5) inferior fronto-occipital fasciculus. Mean indexes values of the predefined ROIs were obtained to perform statistical analyses in SPSS.

2.6. Statistical analysis

Normality of data was tested, using the Kolmogorov–Smirnov test. Between-group differences were compared, using the two-tailed t-test or χ^2 test including as covariates age, gender and education. Pearson's partial correlations, including as covariates age, gender, education, LEDD, UPDRS III, Hoehn and Yahr stage and disease duration were performed in PD. Pearson's partial correlations, including as covariates age, gender and education were performed in HC. Two outliers were excluded for correlation analyses in PD group using boxplots to avoid false correlations. Finally, a hierarchical multiple regression analysis was conducted to examine if the age, GM atrophy, as well as WM alteration predicted the FC differences between the regions of the DMN in PD patients. The predictor variable of age was entered in the first block because disrupted connectivity in aging persists even controlling for brain

atrophy or age-related structural changes [25] and because age demonstrated the importance in DMN alterations and its impact on memory [15]; the predictor variables of GM atrophy correlates were entered in the second step, the final predictor variables of WM alteration correlates were entered in the third block. The criterion variable was FC differences. To obtain adjusted mean differences in change scores and correlations, we used bootstrapping. Effect size (Cohen's *d* and 95% confidence interval [CI]) was calculated, based on the change in the score differences between groups. Cohen's *d* values of 0.20, 0.50 and 0.80 were considered small, medium and large, respectively. Bonferroni's correction for multiple comparisons was not applied because of the exploratory nature of the study and the low sample size. Statistical analyses were performed, using the statistical package SPSS program (IBM SPSS Statistics 23).

3. Results

3.1. Resting-state, cognitive and brain anatomical differences

3.1.1. Resting-state FC

The seed-based FC with a seed in the PCC was significantly decreased in the left and right MTL in PD patients compared with HC (Fig. 1). No differences were found in the other located seeds. The same analysis without LEDD as covariate only revealed significant decreased between PCC and right MTL ($p = 0.042$).

3.1.2. Cognition

PD patients showed significantly decreased processing speed, verbal fluency, verbal and visual memory, visual abilities and executive function performance, compared with HC [see Table S1 in Supplementary Materials (SM)].

3.1.3. GM volume

PD patients showed significantly decreased volume in the ACC, PCC, precuneus, left MTL and bilateral IPC, compared with HC (see Table S2 in SM).

3.1.4. WM indexes

PD patients showed significantly reduced FA in the corpus callosum body, anterior cingulate fasciculus, inferior fronto-occipital fasciculus, inferior longitudinal fasciculus and right posterior cingulate fasciculus, compared with HC (see Table S3 in SM). No significant differences were found between groups in AD, MD and RD indexes.

3.2. Cognitive and brain anatomical correlates between the regions of the DMN

FC between the PCC and left MTL correlated with verbal and visual memory, whereas FC between the PCC and right MTL correlated with visual abilities (see Table S4 in SM, Fig. 2). Regarding GM volume correlates, FC between the PCC and left MTL correlated with the GM volume of the PCC and precuneus in PD patients (see Table S4 in SM, Fig. 3). Finally, FC between the PCC and MTL correlated with WM FA of the right inferior longitudinal fasciculus and right posterior cingulate fasciculus in PD patients (see Table S4 in SM, Fig. 3). No significant correlations were found in HC group between FC differences and cognition, GM or WM data (see S5 in SM).

3.3. Post-hoc analyses in PD patients

3.3.1. FC differences controlling for GM

After controlling for GM atrophy, the FC differences between PCC and left MTL (cluster size = 161, $p = 0.020$) and right MTL (cluster size = 136, $p = 0.020$) remained significant.

3.3.2. Cognitive correlates of GM and WM

Visual memory correlated with GM of posterior cingulate cortex ($r = 0.450$, $p = 0.014$), precuneus ($r = 0.524$, $p = 0.004$), left medial temporal lobe ($r = 0.371$, $p = 0.047$) and right parietal ($r = 0.374$, $p = 0.046$). Verbal memory correlated with anterior ($r = 0.475$, $p = 0.009$) and posterior cingulate cortex ($r = 0.687$, $p < 0.001$) and

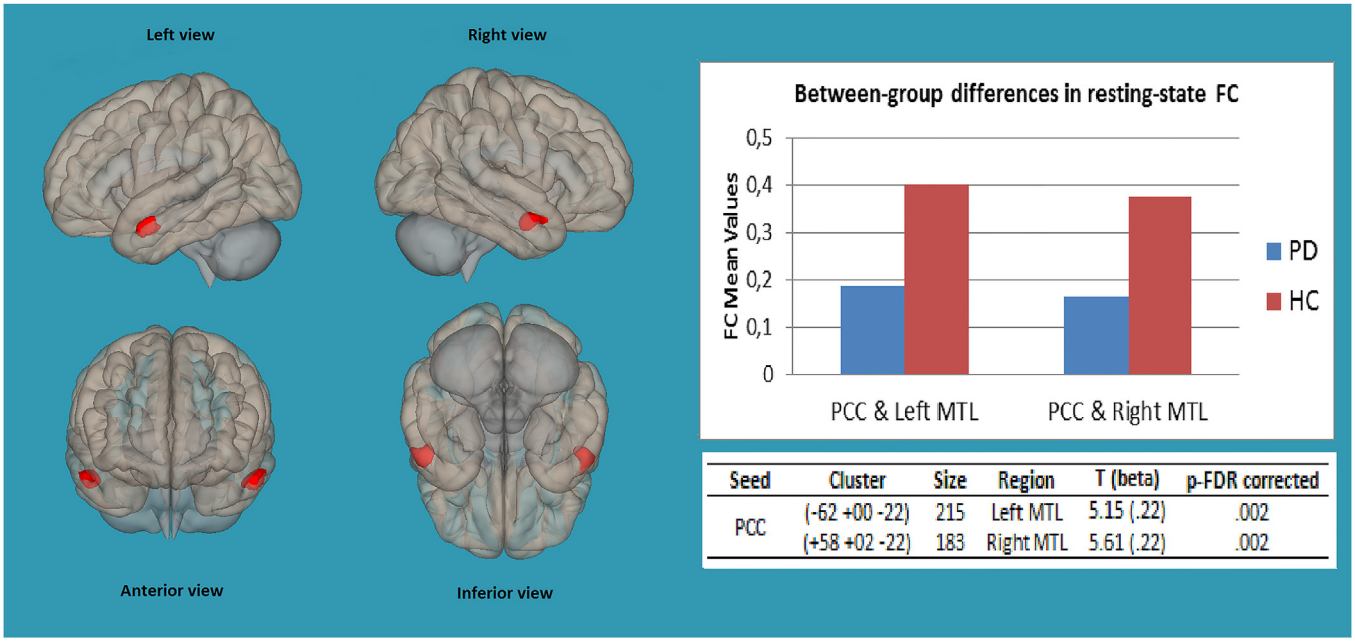

Seed	Cluster	Size	Region	T (beta)	p-FDR corrected
PCC	(-62 +00 -22)	215	Left MTL	5.15 (.22)	.002
	(+58 +02 -22)	183	Right MTL	5.61 (.22)	.002

Fig. 1. Between-groups differences in resting-state FC between the regions of the DMN. Legend: DMN functional connectivity (FC) differences between PD patients and HC. PD patients showed significantly reduced FC between the PCC and bilateral MTL, compared with HC. Cluster-level inference at p(FWE) < 0.05 at a height threshold of p(uncor) < 0.001. Seed located in the PCC. PD = Parkinson's disease; HC = Healthy controls; FC = Functional connectivity; DMN = Default mode network; PCC = Posterior cingulate cortex; MTL = Medial temporal lobe.

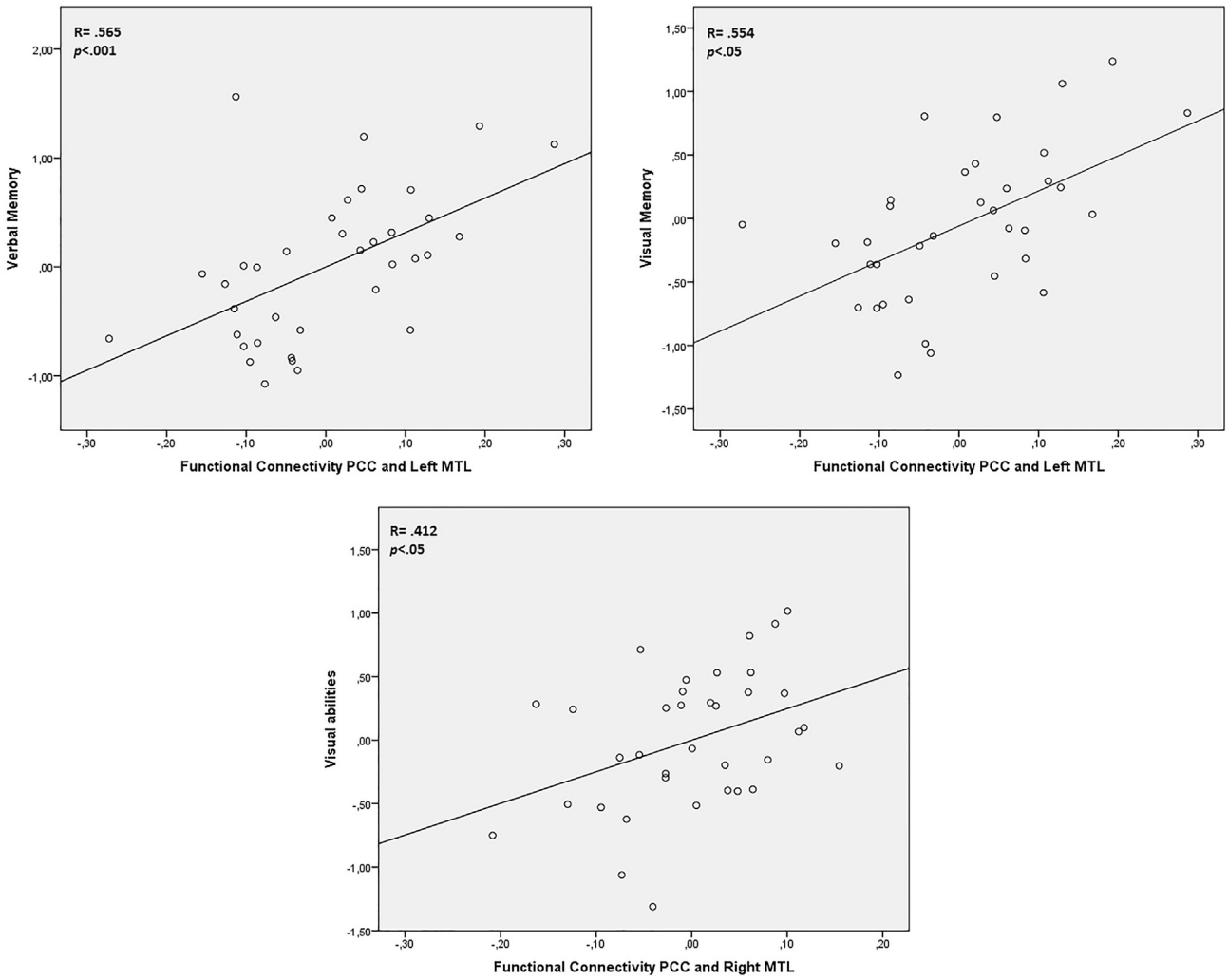

Fig. 2. Significant cognitive correlates of the DMN in PD patients. Legend: PD = Parkinson's disease; DMN = Default mode network; PCC = Posterior cingulate cortex; MTL = Medial temporal lobe.

precuneus (r = 0.659, $p < 0.001$). Finally, visual abilities correlated with GM of posterior cingulate cortex (r = 0.427, $p = 0.023$) and precuneus (r = 0.394, $p = 0.038$). No correlations were found between cognitive measures and WM FA differences.

3.3.3. *Cognitive correlates of FC controlling for GM*

Controlling for the GM regions which correlated with cognitive composites, cognitive correlates of FC differences also remained significant in verbal memory (r = 0.446, $p = 0.023$), visual memory (r = 0.481, $p = 0.017$) and visual abilities (r = 0.441, $p = 0.024$).

3.3.4. *Hierarchical regression of brain atrophy and FC differences between the regions of DMN in PD*

No strong relationships were observed between the predictor variables. VIF values (<10) and tolerance values (>0.1) for all predictor variables were also adequate, thereby demonstrating that there was no issue with multicollinearity. Age failed to add significantly to the FC differences. The result of this analysis showed that the overall model was significant explaining 21% of the variance in FC differences in PD patients ($F(4, 32) = 3.35$, $p = 0.021$) being WM FA alterations the strongest predictor of FC in PD.

4. Discussion

The present study aimed to investigate resting-state FC between the regions of the DMN and explored the cognitive and brain anatomical correlates of the DMN disruption in PD, by combining cognitive data and a multimodal neuroimaging approach. Two main findings were obtained. First, this study revealed significant FC reduction between the regions of the DMN (PCC and bilateral MTL) in PD. Second, the observed DMN disruption was associated with decreased cognitive performance, GM volume and WM FA in PD.

Previous studies suggested dysfunction in several areas of the DMN regions in PD by detecting alterations in posterior midline areas [9,11]. In addition, other studies reported decreased DMN connectivity specifically in the MTL and IPC [10,11]. In relation to our first objective, our imaging data indicated a decreased FC between the PCC and bilateral MTL regions in PD which disappeared without LEDD as covariate. Although there are different published approaches to analyzing resting-state fMRI in PD [26], it is clear that dopamine plays a critical role in the functional reorganization of the brain [27], therefore, we used LEDD as a covariate. In our study, in addition to alterations in the posterior–temporal FC, PD patients exhibited GM volume loss in DMN areas, mainly in posterior

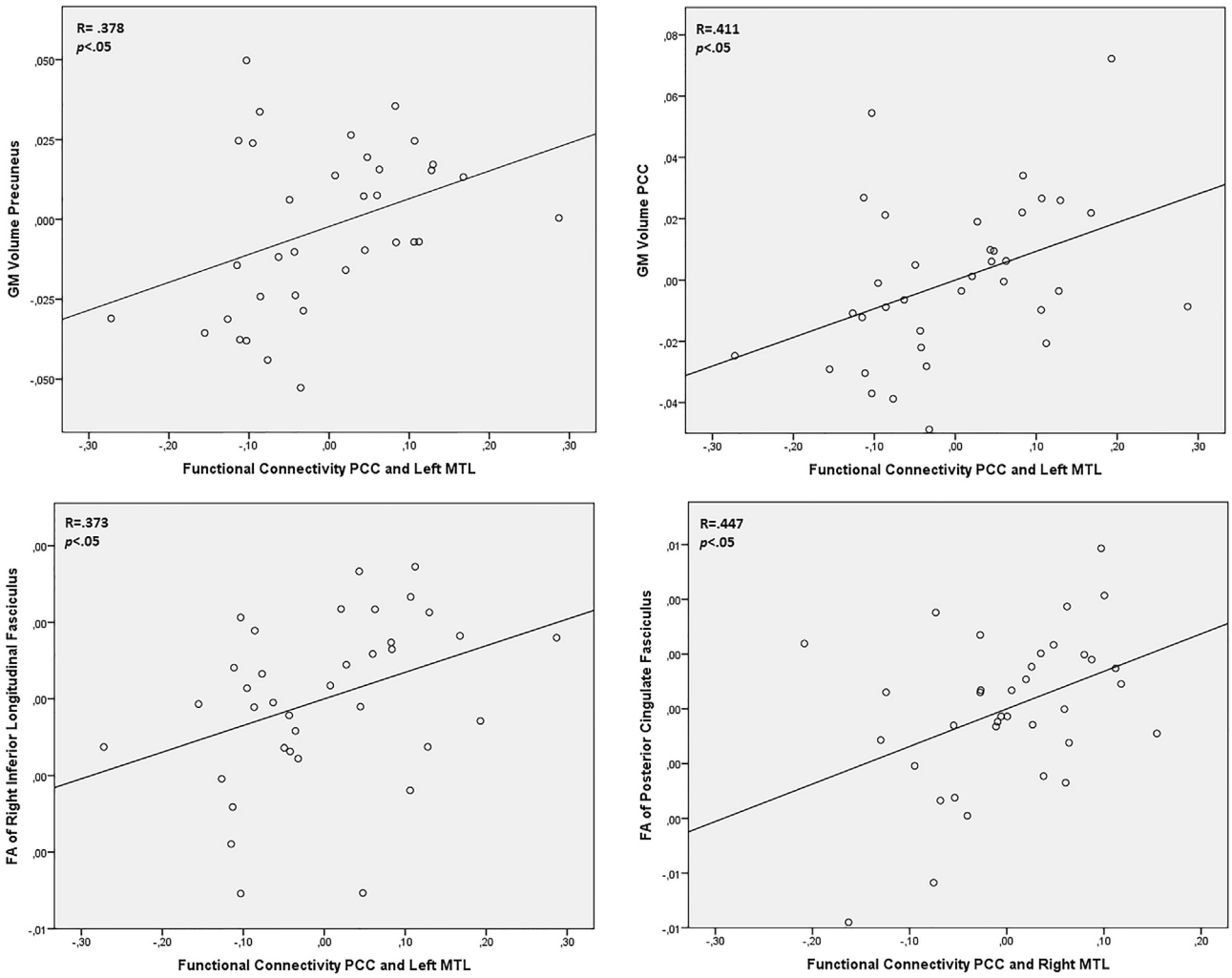

Fig. 3. Significant brain GM volume and WM FA correlates of the DMN in PD patients. Legend: PD = Parkinson's disease; GM = Gray matter; WM = White matter; FA = Fractional anisotropy; DMN = Default mode network; PCC = Posterior cingulate cortex; MTL = Medial temporal lobe.

midline areas, and WM FA degeneration adjacent to those DMN areas. Although PD patients exhibited GM atrophy, the FC differences between the regions of the DMN remained significant even after controlling for GM atrophy, suggesting that FC differences between the regions of the DMN were not GM volume dependent.

For our second objective, we investigated whether the DMN alteration was associated with cognitive and brain anatomical data. Although previous studies of the DMN resting-state have correlated FC with cognitive performance and GM volume [11,12], little is known about WM correlates. We found that the FC disruption between the PCC and left MTL was associated with verbal and visual memory impairment, whereas the FC disruption between the PCC and right MTL was associated with deterioration in visual abilities. These two findings are in line with previous works which also demonstrated a relationship between DMN connectivity and cognitive functions such as memory and visuospatial processing [4,11,12,14]. Furthermore, dysfunctions of the DMN predict cognition in PD [28], are associated with memory and visuospatial abilities in PD [11,12] and precede recognition memory deficits in early PD [14]. In terms of GM volume correlates, we found that the FC disruption between the PCC and left MTL was associated with GM atrophy of the PCC and precuneus. Our results revealed lower FC between these regions of the DMN and lower GM volume in the posterior regions, suggesting that the posterior DMN is the most affected area in PD. These results are also supported by some studies that revealed that the PCC, included in the DMN, is connected to the temporal cortex and linked to memory functions [29]. Finally, and as a novel approach, in relation to WM correlates, the DMN disruption between the PCC and right MTL was associated with a decrease in WM FA of the right posterior cingulate fasciculus in PD. A previous study showed that the pattern of DMN FC was significantly associated with the WM microstructure in the cingulate bundle [24]. Moreover, a positive association was also found between DMN disruption of the PCC and left MTL and WM FA of the right inferior longitudinal fasciculus, a fiber bundle that has been previously associated with the connection between the PCC and MTL [30]. These results suggested that posterior cingulate alteration is present also in WM microstructure and is associated with disruption of the FC in PD.

To further interpret the DMN FC correlates in PD patients a hierarchical regression was used. The overall model combining brain GM and WM correlates was the best predictor of FC differences between PCC and left MTL in PD patients. The analysis suggested that the FC alteration between the regions of the DMN is not only related to GM atrophy but also to alterations in WM adjacent regions. This model confirms that DMN FC disruption was related to

GM and WM brain atrophy in cognitively impaired PD patients.

Our study has some limitations that would need to be considered. First, our results are based on cross-sectional data. Therefore, further longitudinal studies are required to confirm our findings. Second, the sample size is relatively small, and, as such, our results have to be considered as preliminary; nevertheless, our results survived for bootstrapping and reached a high effect size demonstrating the clinically relevance of the results. Third, our results need to be interpreted with caution, since we did not compare "ON/OFF" conditions.

Finally, the strength of this study was that we assessed resting-state fMRI DMN in combination with T1-weighted and diffusion-weighted images and with a cognitive battery. Thus, this combined approach allowed us to examine all aspects of the DMN simultaneously. To the best of our knowledge, our study is the first to demonstrate that DMN alteration in PD is associated with a defined and focal pattern of brain GM volume and WM FA abnormalities centered on the PCC and subsequent connections to the MTL, which revealed a lower performance in memory and visual abilities. This study highlights the close relationship between functional and anatomical changes and its effect on cognitive performance. In conclusion, the study supports that the FC alteration between the regions of the DMN is not only related to GM atrophy but also to alterations in WM adjacent regions and highlights the importance of investigating PD using a multimodal approach.

Funding sources

This study was supported by the Health Department of the Basque Government (2011111117; to Dr. Naroa Ibarretxe Bilbao) and the Spanish Ministry of Economy and Competitiveness (PSI2012-32441; to Dr. Naroa Ibarretxe Bilbao).

Conflicts of interest

Nothing to report.

Acknowledgments

We would like to thank ASPARBI and all of the participants involved in the study for making this research possible.

Appendix A. Supplementary data

Supplementary data related to this article can be found at http://dx.doi.org/10.1016/j.parkreldis.2016.09.012.

References

[1] M.A. Hely, W.G.J. Reid, M.A. Adena, G.M. Halliday, J.G.L. Morris, The Sydney Multicenter Study of Parkinson's disease: the inevitability of dementia at 20 years, Mov. Disord. (2008), http://dx.doi.org/10.1002/mds.21956.

[2] A.J. Yarnall, D.P. Breen, G.W. Duncan, T.K. Khoo, S.Y. Coleman, M.J. Firbank, et al., Characterizing mild cognitive impairment in incident Parkinson disease the ICICLE-PD Study, Neurology 82 (2014) 308–316.

[3] T.R. Melzer, R. Watts, M.R. Macaskill, T.L. Pitcher, L. Livingston, R.J. Keenan, et al., White matter microstructure deteriorates across cognitive stages in Parkinson disease, Neurology 80 (2013) 1841–1849, http://dx.doi.org/10.1212/WNL.0b013e3182929f62.

[4] O. Lucas-Jiménez, M. Díez-Cirarda, N. Ojeda, J. Peña, A. Cabrera-Zubizarreta, N. Ibarretxe-Bilbao, Verbal memory in Parkinson's disease: a combined DTI and fMRI study, J. Park. Dis. 5 (2015) 793–804, http://dx.doi.org/10.3233/JPD-150623.

[5] O. Monchi, M. Petrides, B. Mejia-Constain, A.P. Strafella, Cortical activity in Parkinson's disease during executive processing depends on striatal involvement, Brain 130 (2007) 233–244, http://dx.doi.org/10.1093/brain/awl326.

[6] E. Mak, L. Su, G.B. Williams, J.T. O'Brien, Neuroimaging correlates of cognitive impairment and dementia in Parkinson's disease, Park. Relat. Disord. 21 (2015) 862–870.

[7] A.S. Choe, C.K. Jones, S.E. Joel, J. Muschelli, V. Belegu, B.S. Caffo, et al., Reproducibility and temporal structure in weekly resting-state fMRI over a period of 3.5 years, PLoS One 10 (2015) e0140134.

[8] R.L. Buckner, J.R. Andrews-Hanna, D.L. Schacter, The brain's default network: anatomy, function, and relevance to disease, Ann. N. Y. Acad. Sci. (2008), http://dx.doi.org/10.1196/annals.1440.011.

[9] M. Amboni, A. Tessitore, F. Esposito, G. Santangelo, M. Picillo, C. Vitale, et al., Resting-state functional connectivity associated with mild cognitive impairment in Parkinson's disease, J. Neurol. 262 (2014) 425–434, http://dx.doi.org/10.1007/s00415-014-7591-5.

[10] E.A. Disbrow, O. Carmichael, J. He, K.E. Lanni, E.M. Dressler, L. Zhang, et al., Resting state functional connectivity is associated with cognitive dysfunction in non-demented people with Parkinson's disease, J. Park. Dis. 4 (2014) 453–465, http://dx.doi.org/10.3233/JPD-130341.

[11] A. Tessitore, F. Esposito, C. Vitale, G. Santangelo, M. Amboni, A. Russo, et al., Default-mode network connectivity in cognitively unimpaired patients with Parkinson disease, Neurology 79 (2012) 2226–2232, http://dx.doi.org/10.1212/WNL.0b013e31827689d6.

[12] H.C. Baggio, B. Segura, R. Sala-Llonch, M.J. Marti, F. Valldeoriola, Y. Compta, et al., Cognitive impairment and resting-state network connectivity in Parkinson's disease, Hum. Brain Mapp. 36 (2015) 199–212, http://dx.doi.org/10.1002/hbm.22622.

[13] L. Krajcovicova, M. Mikl, R. Marecek, I. Rektorova, The default mode network integrity in patients with Parkinson's disease is levodopa equivalent dose-dependent, J. Neural Transm. (2012), http://dx.doi.org/10.1007/s00702-011-0723-5.

[14] N. Ibarretxe-Bilbao, M. Zarei, C. Junque, M.J. Marti, B. Segura, P. Vendrell, et al., Dysfunctions of cerebral networks precede recognition memory deficits in early Parkinson's disease, Neuroimage (2011), http://dx.doi.org/10.1016/j.neuroimage.2011.04.049.

[15] F. Sambataro, V.P. Murty, J.H. Callicott, H.-Y. Tan, S. Das, D.R. Weinberger, et al., Age-related alterations in default mode network: impact on working memory performance, Neurobiol. Aging 31 (2010) 839–852.

[16] F. Agosta, M. Pievani, C. Geroldi, M. Copetti, G.B. Frisoni, M. Filippi, Resting state fMRI in Alzheimer's disease: beyond the default mode network, Neurobiol. Aging 33 (2012) 1564–1578.

[17] F. Bai, Z. Zhang, H. Yu, Y. Shi, Y. Yuan, W. Zhu, et al., Default-mode network activity distinguishes amnestic type mild cognitive impairment from healthy aging: a combined structural and resting-state functional MRI study, Neurosci. Lett. 438 (2008) 111–115.

[18] S. Whitfield-Gabrieli, A. Nieto-Castanon, A functional connectivity toolbox for correlated and anticorrelated brain networks, Brain Connect. 2 (2012) 125–141, http://dx.doi.org/10.1089/brain.2012.0073.

[19] A. Weissenbacher, C. Kasess, F. Gerstl, R. Lanzenberger, E. Moser, C. Windischberger, Correlations and anticorrelations in resting-state functional connectivity MRI: a quantitative comparison of preprocessing strategies, Neuroimage 47 (2009) 1408–1416, http://dx.doi.org/10.1016/j.neuroimage.2009.05.005.

[20] G. Douaud, S. Smith, M. Jenkinson, T. Behrens, H. Johansen-Berg, J. Vickers, et al., Anatomically related grey and white matter abnormalities in adolescent-onset schizophrenia, Brain 130 (2007) 2375–2386.

[21] S.M. Smith, M. Jenkinson, M.W. Woolrich, C.F. Beckmann, T.E.J. Behrens, H. Johansen-Berg, et al., Advances in functional and structural MR image analysis and implementation as FSL, Neuroimage 23 (2004), http://dx.doi.org/10.1016/j.neuroimage.2004.07.051.

[22] D.K. Jones, M. Cercignani, Twenty-five pitfalls in the analysis of diffusion MRI data, NMR Biomed. 23 (2010) 803–820.

[23] S.M. Smith, M. Jenkinson, H. Johansen-Berg, D. Rueckert, T.E. Nichols, C.E. Mackay, et al., Tract-based spatial statistics: Voxelwise analysis of multi-subject diffusion data, Neuroimage 31 (2006) 1487–1505, http://dx.doi.org/10.1016/j.neuroimage.2006.02.024.

[24] S.J. Teipel, A.L.W. Bokde, T. Meindl, E. Amaro, J. Soldner, M.F. Reiser, et al., White matter microstructure underlying default mode network connectivity in the human brain, Neuroimage (2010), http://dx.doi.org/10.1016/j.neuroimage.2009.10.067.

[25] L.K. Ferreira, G.F. Busatto, Resting-state functional connectivity in normal brain aging, Neurosci. Biobehav. Rev. 37 (2013) 384–400.

[26] J. Prodoehl, R.G. Burciu, D.E. Vaillancourt, Resting state functional magnetic resonance imaging in Parkinson's disease, Curr. Neurol. Neurosci. Rep. (2014), http://dx.doi.org/10.1007/s11910-014-0448-6.

[27] M. Tahmasian, L.M. Bettray, T. van Eimeren, A. Drzezga, L. Timmermann, C.R. Eickhoff, et al., A systematic review on the applications of resting-state fMRI in Parkinson's disease: does dopamine replacement therapy play a role? Cortex (2015) http://dx.doi.org/10.1016/j.cortex.2015.08.005.

[28] O. Dubbelink, M.M. Schoonheim, J.B. Deijen, J.W.R. Twisk, F. Barkhof, H.W. Berendse, Functional connectivity and cognitive decline over 3 years in Parkinson disease, Neurology 83 (2014), http://dx.doi.org/10.1212/WNL.0000000000001020.

[29] M.D. Greicius, K. Supekar, V. Menon, R.F. Dougherty, Resting-state functional connectivity reflects structural connectivity in the default mode network, Cereb. Cortex (2009), http://dx.doi.org/10.1093/cercor/bhn059.

[30] M. Catani, M.T. De Schotten, A diffusion tensor imaging tractography atlas for virtual in vivo dissections,, Cortex 44 (2008) 1105–1132.